Molecular mechanisms of planktonic cellular aggregation in *Burkholderia multivorans*

Mirela Rodrigues Ferreira, IBB - Institute for Bioengineering and Bioscience, Instituto Superior Técnico

Abstract. Bacteria can proliferate as planktonic cells or as sessile communities. One example of these communities are biofilms, in which cells are attached to a surface or can form non-attached planktonic cellular aggregates. The formation of planktonic cellular aggregates is of relevance in natural environments, but also during interaction with host cells resulting in pathogenicity. In patients with cystic fibrosis (CF), microorganisms from the *Burkholderia cepacia* complex and *Pseudomonas aeruginosa* can form such planktonic cellular aggregates and often establish a chronic infection. Although some molecular mechanisms involved in the formation of planktonic cellular aggregates in bacteria are known, in *Burkholderia cepacia* complex, these mechanisms remain poorly understood. For that reason, it was used a *Burkholderia multivorans* cystic fibrosis isolate to construct a transposon mutant library. About 900 mutants were screened and 13 of them selected due to their distinct aggregation phenotype. Each of these mutants was characterized concerning phenotypes such as surface-attached biofilm formation, motility, exopolysaccharide production, growth rates in synthetic cystic fibrosis medium, and virulence in *Galleria mellonella*. Although it was impossible to establish a linear relationship between each phenotype and the aggregation phenotype, it was still possible to identify probable players involved in the formation of aggregates. Among these players are intracellular messengers, transcriptional regulators, ribosomal proteins, membrane proteins, and proteins involved in lipid metabolism.

Introduction

Bacteria can form sessile multicellular communities or live as free living. Such sessile communities are known as biofilms (1). In biofilms, cells are attached to a surface while planktonic cellular aggregates are non-surface attached. The formation of planktonic cellular aggregates is of relevance in natural environments, but also during interaction with host cells resulting in pathogenicity. In patients with cystic fibrosis (CF), microorganisms of the *Burkholderia cepacia* complex (*Bcc*) and *Pseudomonas aeruginosa* can form such planktonic cellular aggregates and often establish chronic lung infections (2, 3).

Cystic fibrosis is the most common lethal genetic disease in Caucasians and is caused by mutations in a gene encoding the cystic fibrosis transmembrane conductance regulator (CFTR) protein (4). CFTR protein functions as a channel for some ions and is found in the apical membranes of epithelial cells, leading to the characteristic of multiorgan disease associated with cystic fibrosis (5).

In case of CF lungs, both *P. aeruginosa* and *Burkholderia cepacia* complex (*Bcc*) bacteria are associated with declining clinical status and a final fatal deterioration of the lungs (2, 6). For this reason, it became relevant to understand the molecular mechanisms behind the formation of these multicellular structures in these bacteria.

P. aeruginosa, in addition of being one of the most problematic microorganisms in cystic fibrosis, is one of the model organisms for the study of cellular aggregates and biofilms. Thus, there is some information about the molecular mechanisms used in the formation of these multicellular structures. These molecular mechanisms include regulation of alginate biosynthesis, metabolic adaptations, and regulation of quorum sensing system, among others (7, 8).

Although *Burkholderia cepacia* complex can form small aggregates in CF lungs, the mechanisms involved in this process in these microorganisms remain poorly understood. The approach includes the use of a *Burkholderia multivorans* cystic fibrosis isolate able to form cellular aggregates to construct a transposon mutant library, followed by screening to identify different abilities to form cellular aggregates. After identification of mutated genes, it will be characterized the effect of each mutation not only in cellular aggregation, but also in other phenotypes such as surface-attached biofilm formation, motility, exopolysaccharide production, growth rates in synthetic cystic fibrosis medium and virulence in *Galleria mellonella*. The aim is to understand not only the genes involved in cellular aggregates formation, but also whether aggregates formation impacts other phenotypes. Identification of key players in this aggregation trait may provide a comprehensive view of genetic pathways to chronic infections, which might lead in the future to different therapeutic intervention and improvement of CF patient's health.

Materials and methods

Bacterial strains and growth conditions

Bacterial strains and plasmids used in this study are listed in Table S1. *E. coli* was grown at 37ºC in Lennox Broth (LB) with or without agar, supplemented with kanamycin (50 µg/ml) or chloramphenicol (25 µg/ml) when required to maintain selective pressure. *Burkholderia multivorans* strains were grown in LB or in SM medium (12.5 g/l $Na_2HPO_4.2H_2O$, 3 g/l KH_2PO_4, 1 g/l K_2SO_4, 1 g/l NaCl, 0.2 g/l $MgSO_4.7H_2O$, 0.01 g/l $CaCl_2.2H_2O$, 0.001 g/l $FeSO_4.7H_2O$, 1 g/l yeast extract, 1 g/l casamino acids, pH 7.2), supplemented with 20 g/l of D-mannitol and kanamycin (500 µg/ml) when required to maintain selective pressure, at 37ºC with 180 rpm of orbital agitation.

DNA manipulation and cell transformation techniques

Genomic DNA from *B. multivorans* strains was extracted using a protocol previously described (9). Plasmid DNA isolation and purification, DNA restriction, agarose gel electrophoresis, DNA amplification by PCR, and *E. coli* transformation were performed using standard procedures (primers are described in Table S2) (10).

Transposon mutant library construction

A transposon mutant library of the clinical isolate *B. multivorans* P0213-1 was generated by triparental mating with E. coli carrying pRK600 (helper) or carrying pTn*Mod*Ωkm (donor) (Fig. S1). The donor strain was inoculated in 3 mL of LB with kanamycin, while the helper strain was inoculated in 3 mL of LB with chloramphenicol and the recipient strain was inoculated in 3 mL of LB. The three cultures were incubated at 37ºC with orbital agitation (250 rpm) for 5 hours. Following incubation, 1 mL of recipient was mixed with 1 mL of each helper and donor. The final mixture was transferred to a LB plate at 30ºC for 24 hours. This conjugation mixture was, then resuspended in 1ml of LB and plated onto 10 LB plates supplemented with 500 µg/ml kanamycin and 40 µg/ml gentamicin, each of them with 100 µl. All were incubated at 37ºC for 24 hours. The mutant colonies obtained were inoculated into each well of 96-well plates and frozen at -80ºC with 30% of glycerol. The mutant colonies were numbered, as for example, A5 (mutant of cystic fibrosis isolate P0213-1 from well 5 of plate A).

Screening of transposon insertion libraries for differences in planktonic cellular aggregates formation

Each bacterial mutant was grown overnight in 3 mL of SM medium at 37ºC with 250 rpm of orbital agitation. Suspensions with OD_{640nm} 0.1, were prepared in fresh SM medium and incubated at 37ºC with 180 rpm of orbital agitation for 48 hours. After this time, each mutant was observed macroscopically and microscopically for aggregates and compared with wild type (P0213-1) strain.

Microscopy analysis

B. multivorans strains grown in SM medium for 48 hours were visualized on Zeiss Axioplan microscope, equipped with a Axiocam 503 color Zeiss camera, using a 10x 0.3 NA objective, and controlled with the Zen software.

Identification of the genes disrupted by the plasposon

The insertion position of the plasposon was determined in the selected mutants by digesting genomic DNA with EcoRI, followed by fragment self-ligation. Then, ligation mixtures were electroporated into *E. coli* and plated in LB supplemented with kanamycin. Plasmids recovered where then sequenced using primer kmR and oriR (Table S2).

In silico *analysis of nucleotide sequences*

The algorithm BLAST (11) was used to compare sequences of the gene disrupted to database sequences available at the National Center for Biotechnology Information (NCBI).

Growth curves and doubling time estimation

Cells from an overnight culture were inoculated in 50 mL of fresh LB, SM medium or SCFM (synthetic cystic fibrosis medium) (12) (OD_{640nm} 0.1). The culture was incubated at 37ºC with 180 rpm of orbital agitation. OD_{640nm} readings were taken over time for 8 hours and then at 23 and 24 hours. Growth rates were calculated from the exponential phase of growth from at least two independent experiments. The doubling time was calculated from the growth rate of the exponential growth phase.

Transposon mutants complementation

For functional complementation of transposon mutants, parental upstream promoter region and respective gene were cloned into the pBBR1MCS broad-host-range vector. Each gene and respective promotor were amplified from the genomic DNA of the wild-type strain (*B. multivorans* P0213-1), previously extracted and purified using the DNeasy® blood and tissue kit (Qiagen®), by PCR, using a set of forward and reverse primers (Table S2) that included engineered restriction endonuclease sites. When the upstream promoter region and gene are amplified individually, the PCR products, after purification with DNA Clean & Concentrator™ kit (Zymoresearch®), were first cloned into pUK21 vector. The PCR products, as well as the pUK21 vector, were then digested by the same restriction endonucleases followed by ligation. Then, ligation mixtures were electroporated into *E. coli* electrocompetent cells using a Bio-Rad Gene Pulser II system (400 Ω, 25 µF, 2.5 kV) and grown for 1 hour before being plated on LB supplemented with kanamycin plus X-gal and IPTG for blue/white selection. Plasmids were then recovered using ZR Plasmid Miniprep™-Classic kit (Zymoresearch®), following the manufacturer´s instructions. Recovered plasmids were digested with the restriction enzymes used before, followed by agarose gel electrophoresis to verify the presence of fragments corresponding to the gene and the upstream promoter region. The DNA fragment that comprises the upstream promotor region and the gene was removed from pUK21 and cloned into the pBBR1MCS vector through the same process described above for pUK21. In this case, selective medium was LB supplemented with chloramphenicol plus X-gal and IPTG for blue/white selection. Recombinant plasmids obtained were purified, and electroporated into electrocompetent cells of *B. multivorans* P0213-1 and its transposon mutant derivatives using a Bio-Rad Gene Pulser II system (200 Ω, 25 µF, 2.5 kV) and grown for 4 hours before being plated on, LB supplemented with chloramphenicol (250 µg/ml). An empty pBBR1MCS vector was electroporated into *B. multivorans* P0213-1 and its derivative transposon mutants and used as a control for functional complementation. Restoration of wild-type cellular aggregation phenotype was tested by growing the cells carrying empty control vectors or expressing parental genes in the same conditions described above.

Quantification of cellular aggregates and free cells

The growth cultures, after incubation in previously described conditions, were transferred to a 50 mL Falcon tube and centrifuged at 1400 rpm of orbital agitation at 25ºC for 30 seconds. After centrifugation, cell suspensions rested for 10 minutes, thus enabling aggregates still in suspension to settled down. Then, the supernatant was removed by pipetting and placed in a new 50 mL Falcon tube. Suspensions containing aggregates were transferred to 2 mL Eppendorf tubes and, then, after a several quick-spins, it was possible to obtain in a 2 mL Eppendorf tube all cellular aggregates of same mutant strain.

The 50 mL Falcon tube with free cells and growth medium was centrifuged for 10 minutes at 4000 rpm of orbital agitation at 25ºC, allowing the separation of free cells from the growth medium. The resulting pellet was resuspended in 5 mL of growth medium and, then, several centrifugations at 13400 rpm of orbital agitation for 2 minutes were performed in 2 mL Eppendorf tubes, in order to collect all free cells of the isolate. In the end of the procedure, two 2 mL Eppendorf tubes were obtained for each strain. These tubes were opened and placed at 60ºC during at least 72 hours until all cellular aggregates and free cells were dried, presenting a brown color. All 2 mL Eppendorf tubes were weighted before the collection of samples and after samples were dried.

Exopolysaccharide production

YEM (yeast extract mannitol medium) plates containing 4 g/L mannitol, 0.5 g/L yeast extract and 15 g/L agar were used to evaluate the production of exopolysaccharide (13). After inoculation, YEM plates were incubated for 48 h at 37°C and mucoidy due to exopolysaccharide production was observed by visual inspection.

Biofilm formation

Bacteria were grown in LB medium at 37°C to mid-exponential phase and diluted to an OD_{640nm} of 0.05. 200 µL samples of the cell suspensions were used to inoculate 96-well polystyrene microtiter plates. 200 µL of LB medium were used to inoculate some wells functioning as blanks. Plates were incubated at 37°C statically for 48 h, after which the wells were washed three times with 0.9% (wt/vol) NaCl. The biofilm was stained with 200 µL of a 1% (wt/vol) crystal violet solution for 20 minutes at room temperature (14), followed by washing three times with 200 µL of 0.9% (wt/vol) NaCl. The dye was then solubilized with 200 µL of 96% ethanol and the biofilm was quantified by measuring the absorbance of the solution at 590 nm (A_{590nm}) in a microplate reader (Spectrostar nano, BMG LabTech). Results are the means of data from at least six replicates of three independent experiments

Swimming motility

The swimming agar plates containing 1% (wt/vol) tryptone, 0.5% (wt/vol) NaCl, 0.3% (wt/vol) noble agar (Difco) (15) were spot inoculated with a 5 µl drop of a culture at an OD_{640nm} of 1.0. After inoculation, swimming plates were incubated for 24 h at 37°C and the diameter of the swimming zone was measured. Results are the means of data from at least ten replicates of two independent experiments.

Swarming motility

The swarming agar plates containing 0.04% (wt/vol) tryptone, 0.01% (wt/vol) yeast extract, 0.0067% (wt/vol) CaCl2, 0.6% (wt/vol) bacto agar (Difco) (15) were spot inoculated with a 5 µl drop of a culture at an OD_{640nm} of 1.0. After inoculation, swarming plates were incubated for 48 h at 37°C and the diameter of the swarming zone was measured. Results are the means of data from at least ten replicates of two independent experiments.

Virulence determination in Galleria mellonella

Killing assays were performed as described previously (16). *Galleria mellonella* larvae were injected with cell suspensions containing a total CFU of approximately $1x10^4$ in 10 mM MgSO4 with 1.2 mg/ml ampicillin and incubated at 37°C. Survival rates were assessed during the following 3 days post-infection. As a negative control, 10 mM MgSO4 with 1.2 mg/ml ampicillin was used. Ten larvae per isolate were used in at least three independent experiments.

Statistical analyses

The statistical significance of differences in the data was determined using the one-way analysis of variance (ANOVA) followed by Dunnett's multiple comparisons test or Turkey's multiple comparisons test and using the Mantel-Cox test which were performed using GraphPad Prism software v.5.04 for Windows, (GraphPad Software, San Diego California USA, www.graphpad.com). Kaplan-Meier survival curves were also performed with GraphPad Prism software v.5.04. Differences were considered statistically significant for P-values lower than 0.05.

Results and discussion

In vitro *screening of* Burkholderia multivorans *plasposon mutants*

When grown in SM medium, which has high carbon to nitrogen ratio, *B. multivorans* P0213-1 grows both as free cells and cellular aggregates (Fig. 1). These aggregates range from microscopic to macroscopic.
In order to identify the molecular mechanisms involved in the formation of cellular aggregates, it was constructed a plasposon mutant library from P0213-1, using the transposon present in pTn*Mod*ΩKm (Fig. S1). From this plasposon mutant library, about 900 colonies were screened to determine if any presented differences in the formation of cellular aggregates. Both mutants and wild type strain were incubated at 37ºC with 180 rpm of orbital agitation for 48 hours and, then, mutants were visually compared with wild type at macroscopic and microscopic levels.
From the 900 mutants screened, 13 mutants were selected due to their distinct phenotype (Fig. 1). These mutants were grown several times to confirm their different ability to form cellular aggregates

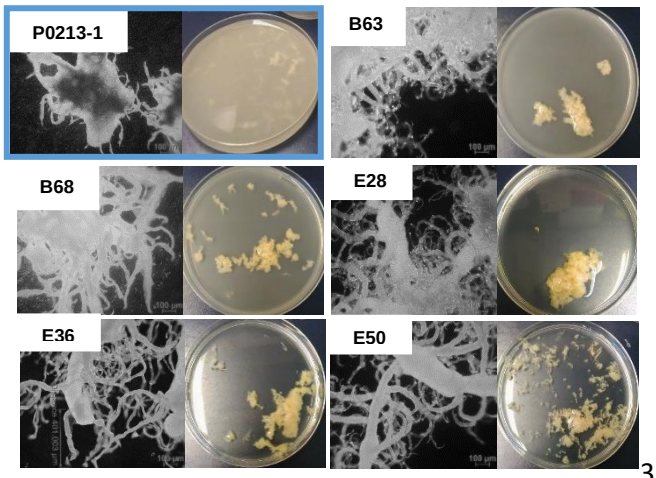

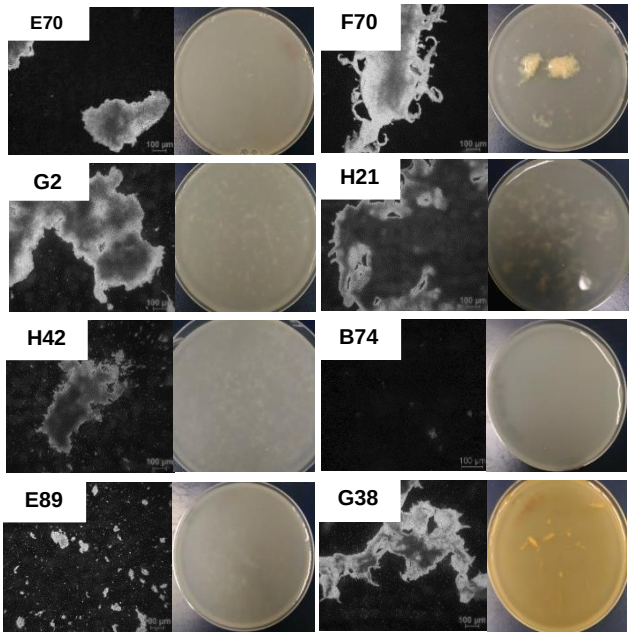

Fig. 1 Screening of the transposon mutant library of *B. multivorans* P0213-1 for different abilities to form planktonic cellular aggregates. For each strain is shown a microscopy image (on the left) and the liquid culture on a petri dish (on the right). Each culture was grown in SM medium at 37ºC, 180 rpm of orbital agitation, for 48 hours.

B63, B68, E28, E36 and E50 mutants produce cellular aggregates that comprise the majority of cells in the culture, as it can be seen from the low turbidity of the medium and the low amount of cells present in microcopy image (Fig. 1). These aggregates seen with 100x magnification are highly structured, showing main branches from where smaller ramifications are protruding. The next group of selected mutants has an intermediate ability of forming cellular aggregates. In this category are included G2, E70, F70, H21, H42. In general, the size of the aggregates is smaller than the ones of the wild-type strain and they are much less structured. In this type of aggregates no significant branching is observed, perhaps with the exception of F70 mutant. The last category of selected mutants includes B74, E89 and G38 mutants. As depicted in figure 1 these mutants produce very few macroscopic aggregates. At the microscopic level, B74 is the one producing smaller aggregates, followed by E89. G38 mutant produces few macroscopic aggregates, but with low structure. Additionally, G38 liquid cultures turn orange while the wild-type and other mutants are white/yellow.

Although it is possible to identify the differences between the size/number of aggregates of the wild-type and the mutants at naked eye, it has become necessary to quantify both aggregates and free cells, in order to determine, the percentage of planktonic cellular aggregates formation of each mutant (Fig. 2).

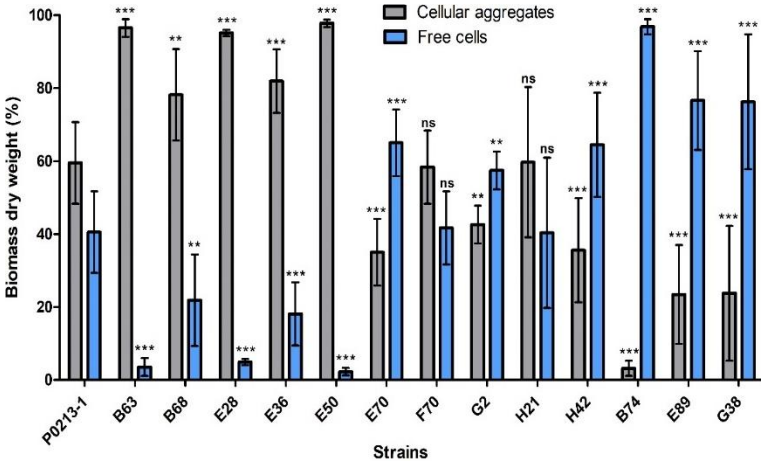

Fig. 2 Quantification of cellular aggregates and free cells of wild-type (P0213-1) and its derivative strains. Error bars correspond to the standard deviations of the mean values of at least four independent experiments. Significance level (one-way ANOVA followed by Dunnett's multiple comparison test) between cellular aggregates and free cells of the wild-type (P0213-1) and cellular aggregates and free cells of the P0213-1 derivative strains was determined: *, P<0.05; ***, P<0.001; ****, P<0.0001; ns, not statistically significant.

The chosen mutants were distributed into three categories (Table 1).

Table 1. Selected mutants divided in three distinct categories.

Percentage of planktonic cellular aggregates		
> 75%	**> 25 % and < 75%**	**<25 %**
B63	P0213-1	B74
B68	F70	E89
E28	H21	G38
E36	E70	-
E50	G2	-
-	H42	-

Identification and analysis of plasposon insertion in the genome of the selected mutants and the possible role of mutates genes in cellular aggregation

Having demonstrated the presence of the plasposon in the genome of the selected mutants (data not shown), the next step was to identify their localization and consequently the disrupted genes.

The followed strategy was the digestion of each genome by a restriction endonuclease unable to cut the plasposon (such as EcoRI) followed by self-ligation and electroporation of these ligations into *E. coli*. Following this procedure, we were able to obtain colonies for mutants' genomes which confirmed the presence of a plasmid with approximately 5 kbp (data not shown). Sanger sequencing of the flanking regions allows the identification of plasposon insertion in the *B. multivorans* mutants' genome.

In silico analysis, through the BLAST algorithm identified the disrupted genes (Table 2).

Table 2. Genes disrupted by the plasposon were identified in the *B. multivorans* selected mutants.

Mutant	Gene annotation
B63	Xanthine dehydrogenase molybdenum binding subunit
B68	Fatty acid metabolism regulator protein
E28	Phosphoenolpyruvate phosphomutase
E36	HTH-type transcriptional repressor NemR
E50	MMPL family protein
E70	Phosphoenolpyruvate synthase
F70	Outer membrane porin protein precursor
G2	HTH-type transcriptional regulator TtgR
H21	ImpA family type VI secretion-associated protein | Type VI secretion protein
H42	Acetyltransferase YpeA
B74	30S ribosomal protein S9
E89	Cytochrome c-552 precursor
G38	Ferredoxin-dependent glutamate synthase 1

Growth properties in LB confirm a very similar growth behavior, both in exponential and stationary phase, between wild-type and all selected mutants (data not shown). Based on that, it was concluded that, under standard conditions, the disrupted genes interfere in the formation of planktonic cellular aggregates without interfering significantly with the growth kinetics.

The gene disrupted in B63 mutant is involved in the purine salvage pathway. This mutant is unable to recycle purine creating a stronger nitrogen limitation and potentiating the formation of aggregates in detriment of free-living cells. Under these conditions, is likely that the levels of alarmone and c-di-GMP are altered (since the GMP/GTP pool is not maintained), which will influence several phenotypic traits (17).

The mutated gene in B68 mutant encodes a transcriptional regulator of the TetR family, which might regulate an operon of four genes. Depending on whether this regulator is a repressor or an activator of the four genes operon, the metabolism could shift between terpenoid biosynthesis and branched chain fatty-acid biosynthesis (18).

Mutated gene of the E28 mutant responsible for converting phosphoenolpyruvate into 2-aminoethylphosphonate (18), which produces pyruvate from phosphonopyruvate in the phosphonate metabolism (19). This pathway is involved in the synthesis of some antibiotics, phosphonolipids, and surfactants. It could be that the absence of phosphonolipids in the membrane or the absence of a putative surfactant alters surface properties of cells, increasing cell aggregation.

E36 mutant has a mutation on a gene encoding a TetR family transcriptional regulator, however, the possible role in aggregation is not known.

The disrupted gene of E50 mutant is within a possible operon with at least 18 genes and these might be in the synthesis of molecules with lipid backbones since some of the gene products are involved in fatty acid synthesis (18).

E70 mutant is disrupted in gene *ppsA* encoding phosphoenolpyruvate synthase, an enzyme converting pyruvate into phosphoenolpyruvate. Probably, due to the block of this conversion, there is an increased of pyruvate and acetyl-CoA and, perhaps, an increase of lipid metabolic reactions. In literature was also found a link between a mutation in this gene and an increase ability to produce N-acyl-homoserine lactones, the signal molecules of the quorum sensing system (20).

F70 mutant has the plasposon inserted into a gene encoding a putative porin. Possibly, it transports some compound important during cell aggregation.

G2 mutant has a disruption in a gene encoding a transcriptional regulator of the TetR family that might regulate genes encoding a putative RND efflux system (21). Without repression, there is a constitutive expression in G2 mutant of the efflux pumps genes in the absence of antibiotics seems to have a negative effect in promoting the growth of cellular aggregates, but the mechanism behind that is unknown.

The recovery of the flanking regions from H21 mutant identified the plasposon in two adjacent location. One disrupts the gene encoding type VI secretion system protein TssA (homologue to Bmul_2923) and the other plasposon is inserted into *tssG* gene encoding another protein of the same secretion system. The type VI secretion system is a bacterial nanomachine used to deliver toxins directly into eukaryotic or prokaryotic target cells (22). The fact that it still forms aggregates but of smaller size implicates this nanomachine in this process.

H42 mutant has the plasposon inserted into the *ypeA* gene encoding a putative acetyltransferase. This gene is the last of a 2-operon structure, being the first gene *argD*, which is involved in the synthesis of N-acetylornitine. Whether ypeA acetyltransferase is also involved in this pathway and how it influences cellular aggregation is unknown.

In B74 mutant plasposon disrupted the *rpsI* gene. This gene encodes the 30S ribosomal protein S9 involved in translation. The most likely hypothesis is that B74 mutant without a functional S9 protein, presents some defects in translation due to the possibility of uncorrected association of 30S and 50S subunits of ribosome and consequently the translation of some transcripts might be affected (23).

E89 mutant has the plasposon inserted in gene *cycA_3* encoding a putative cytochrome c. The gene downstream, possibly from the same operon, encodes an enzyme metabolizing one of the steps of styrene degradation. Since cytochrome c-type proteins are involved in electron transfer, it is possible that one of the steps of this degradative pathway might involve this protein. The role of this pathway in cellular aggregation is unknown.

The last mutant, G38 mutant, has *gltB* gene disrupted, which encodes glutamate synthase protein. In this conditions, based on literature (24), the via GS(glutamine synthase)/GOGAT(glutamate synthase) is the one used to assimilate ammonium in these conditions. Consequently, the intracellular levels of glutamine might increase, once it cannot be used by non-functional GOGAT enzyme, but glutamate is still formed from arginine succinyltransferase (AST) pathway, allowing the continuous assimilation of NH_4^+ substrate (25). Therefore, the possible increase of glutamine levels and the decrease of 2-oxoglutarate levels might lead to the turned off of the NtrBC system. The fact that this mutant still forms

aggregates but of smaller size implicates somehow this Ntr system regulatory pathway in the aggregation process.

Together, mutant analysis seems to indicate that changes in lipid metabolism (and possibly signaling) have positive effect in aggregates formation, while the disruption of genes related with translation and regulation of nitrogen metabolism have a detrimental effect. Having more moderate effects on cellular aggregates we highlight an Omp porin and the type VI secretion system.

Transposon mutants complementation

To confirm the importance of the mutated genes in cell aggregation, *rpsI* gene was cloned in a replicative vector such as pBBR1MCS and complementation of the respective mutant was performed.

The complemented B74 mutant, mutated in *rpsI* gene encoding ribosomal protein S9. Since this gene is in a putative operon together with *rplM* gene, it was cloned the upstream region of *rplM* gene and the *rpsI* gene into pBBR1MCS. This constructed was named PMF18-4. Overexpression of this gene in the wild-type strain did not influence the distribution of biomass between aggregates and free cells (Fig. 3(B)). But, expression of the *rpsI* gene in the mutant increased considerably the aggregates biomass (Fig. 3(B)) and size (Fig. 3(C)). Although, complementation did not reach wild-type levels, this experiment was successful.

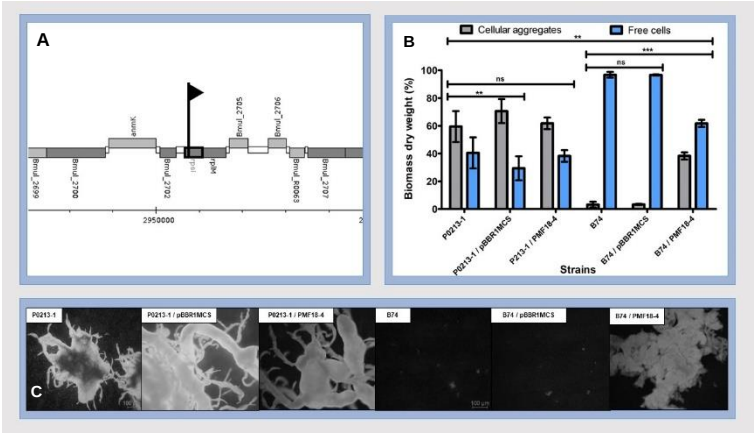

Fig. 3 Complementation of the B74 mutant. (A) Genomic location of the plasposon in *B. multivorans* B74 mutant showing a region from chromosome 1. Together in the same operon is *rplM* gene encoding 50S ribosomal protein L13. Downstream of *rplM* is a gene encoding a hypothetical protein. Upstream is a gene encoding an iron-sulfur cluster insertion protein ErpA**. (B) Quantification of cellular aggregates and free cells of wild-type (P0213-1), mutant and complemented mutant.** Error bars correspond to the standard deviations of the mean values of at least four independent experiments. Significance level (one-way ANOVA followed by Turkey's multiple comparison test) between cellular aggregates and free cells of the wild-type (P0213-1) and cellular aggregates and free cells of the P0213-1 derivative strains was determined: **, P<0.01; ***, P<0.001; ns, not statistically significant. **(C) Microscopic images of wild-type, mutant and complemented mutant.**

In addition to the aggregates phenotypes already described, is our main to identify if other phenotypes are altered as well in the selected mutants. Such traits include surface-attached biofilm formation, antibiotic susceptibility (data not shown), motility, growth and virulence.

Surface-attached biofilm formation

Surface-attached biofilm formation and planktonic cellular aggregates formation share important steps. Thus, in here, we evaluated the ability of each mutant under study to produce surface-attached biofilms (Fig. 4).

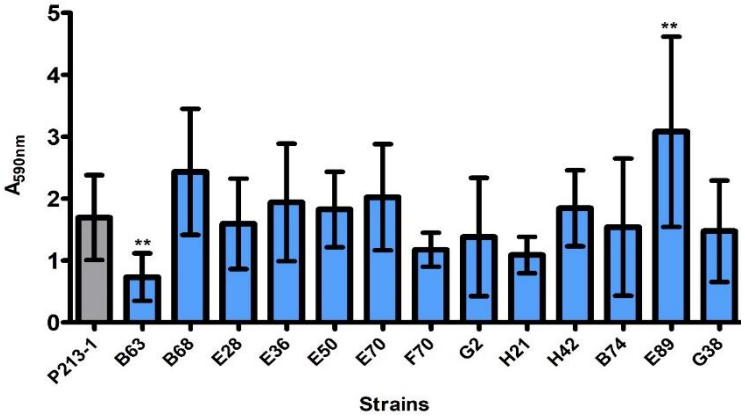

Fig. 4 Surface-attached biofilm formation of the P0213-1 and its derivative mutants was determined by absorbance measurement at 590 nm after growth for 48h at 37ºC in polystyrene microplates. Error bars correspond to the standard deviations of the mean values of at least seven independent experiments. Significance level (one-way ANOVA followed by Dunnett's multiple comparison test) between the wild-type (P0213-1) and the mutants was determined: **, P<0.01

Of all tested mutants only two of them presented statistically significant differences in the surface-attached biofilm formation in comparison with the wild-type. Based on results shown in figure 4, the B63 mutant presented the lower absorbance and the E89 mutant has the highest surface-attached biofilm formation. B63 has the xanthine dehydrogenase molybdenum-binding subunit encoding gene disrupted. As mentioned before this protein is necessary for purine salvage pathway to maintain the GTP levels and, consequently might affect signaling. In a study, a *Burkholderia cenocepacia* H111 mutant, that had a reduced intracellular c-di-GMP level, formed less biofilm when compared to a strain with a high c-di-GMP concentration (26). Taking this into account, perhaps the B63 mutant has altered signaling pathways, resulting in lower biofilm formation. Regarding E89 mutant increased biofilm formation ability, it is difficult to grasp the role of the disrupted gene and therefore everything we might say is speculative.

The opposite results regarding these two phenotypes (planktonic cellular aggregates and surface-attached biofilms) were previously reported in the literature further supporting the results obtain in this study (27, 28). It is important to say, however, that the growth conditions of the different mutants in both experiments were different. These facts must be considered when discussing the differences between these two phenotypes.

Swimming and swarming motility

Motility might be one of the requirements for a successful cellular aggregation, since cellular aggregation depends on contact between bacterial cells through physical forces and biological mechanisms. Thus, motility allows prior approximation of bacterial cells for them to start aggregation (29). To evaluate the motility of the *B. multivorans* strains, swimming and swarming agar plates were incubated for 24 hours and 48 hours, respectively, at 37ºC after inoculation. Then, motility zone diameter (cm) was measured for each of them and the results are present in figure 5.

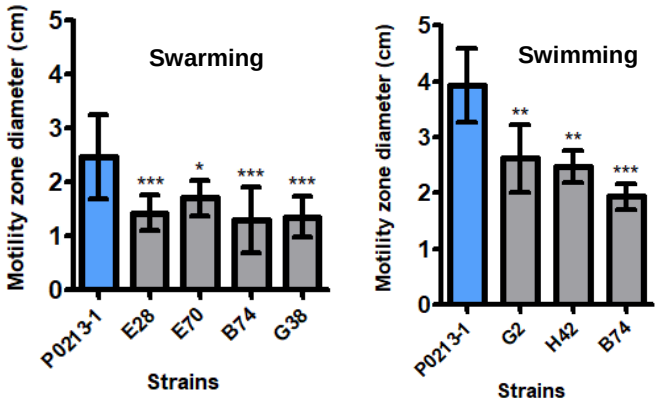

Fig. 5 Swarming and swimming motility of the P0213-1 and some derivative strains was measured as the motility zone diameter after growth at 37ºC. Error bars correspond to the standard deviations of the mean values of at least two independent experiments. Significance level (one-way ANOVA followed by Dunnett's multiple comparison test) between the wild-type (P0213-1) and the mutants was determined: *, P<0.05; **, P<0.01; ***, P<0.001.

Literature search correlating similar mutations as the ones here described and motility did not give useful results. Effectively, only in *Bacillus subtilis* was demonstrated that other two ribosomal proteins (S21 and S11) are important for the regulation of cell motility and biofilm formation (30). These ribosomal protein mutants had shown a decrease in motility, as observed in this study for the B74 mutant. These authors also determined that these two proteins interfere with two major operons that regulates the biofilm formation (30).

The other mutation from which some information is available is the one present in G38 mutant. As mentioned before the G38 mutant presents a non-functional glutamate synthase, which might lead to an increase in the concentration of glutamine and consequently to the inactivation of the NtrBC system. Beyond the *bce-I* and *bce-II* clusters, which produce the EPS cepacian in *Burkholderia*, it was shown that the NtrBC system also regulates swarming motility. Indeed, the swarming ability of the *ntrC* mutant strain was lower than the ability of wild-type and complemented mutant, thus, suggesting that the swarm phenotype of the G38 mutant might be due to negative effects on the Ntr system (31).

Motility is not always necessary for cells prior approximation, since cells can form the initial "seeding" aggregates by random collisions of motile cells or by Brownian motion. However, searching for ideal conditions by bacteria is more advantageous. So, despite the variation observed in some mutations none of them lost motility completely.

Bacteria swim in liquid and swarm over solid surface or in viscous environment. Thus, considering the experimental conditions used, the results of swimming motility are more important to relate motility and the aggregation phenotype. By the results, it is possible to observed that the aggregation was not more than 50% for the strains that shown a statistically significant decrease in swimming motility when compared to the wild-type. However, this is not conserved through all strains tested since some of them present higher aggregation phenotype and less swimming motility than the wild-type.

In the other hand, the swarming motility could be more relevant to ensure surface-attached biofilm formation. But, as demonstrated in swimming motility, the results of swarming motility cannot be correlated to the formation of surface-attached biofilm formation. Together, these results suggest that motility was neither the more important feature for the aggregation phenotype or for surface-attached biofilm formation. It is also important to refer, that there are different mechanisms affecting motility in bacteria and this is highly regulated.

Exopolysaccharide production

Cellular aggregation is mediated by bacterial products, more specifically, extracellular polymeric substances such as polysaccharides, extracellular DNA and ions. In some bacterial species, exopolysaccharides promote the aggregation phenotype (32). Therefore, we also assessed exopolysaccharide production in our mutants (Fig.6).

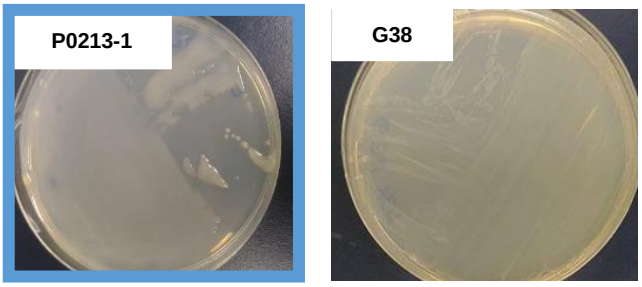

Fig. 6 Evaluation of mucoid phenotype in yeast extract mannitol medium (YEM) after 48 h of incubation at 37°C for wild-type (P0213-1) and G38 mutant.

Figure 6 shows that, except for G38 mutant, all others are highly mucoid in YEM plates (data not shown). The expression of *bce* genes directing the biosynthesis of cepacian are under control of NtrC and σ^{54} in *B. cenocepacia* (24, 31). Since our G38 mutant might have defects in NtrBC signaling, this is possibly the cause of the observed phenotype.

Although cellular aggregation has been shown to be mediated also by exopolysaccharides, there are some antagonistic reports (3, 32). This is also seen in this work, were two mutants (B74 and G38) produce fewer aggregates, but one is mucoid and the other nonmucoid. Another possibility is that cepacian might not have a fundamental role in this process as it has been reported by Silva *et al.* (3), but other polysaccharide produced by these strains might have.

In vitro *growth analysis of selected mutants in synthetic cystic fibrosis medium (SCFM)*

The synthetic cystic fibrosis medium nutritionally mimics cystic fibrosis sputum (12). Since the biofilm formation model described by Worlitsch *et al*. (33) is very similar to the model of planktonic cellular aggregates, it was important to determine if the aggregation phenotype is related to the conditions of growth of the selected mutants (Fig. 7).

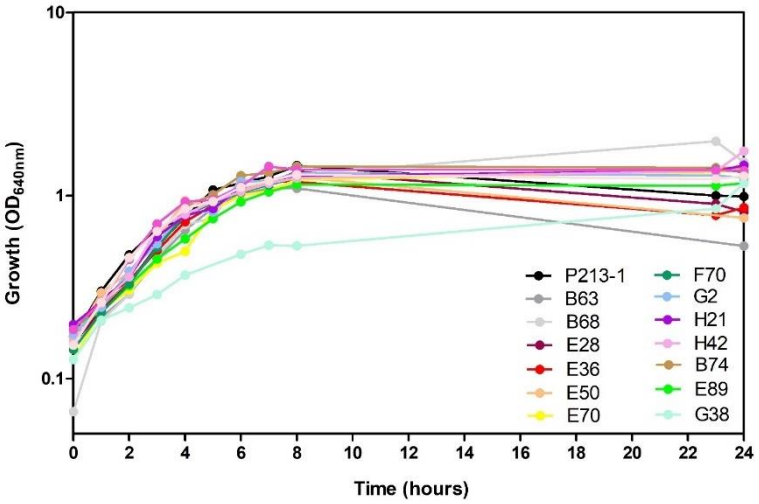

Fig. 7 Growth curves of wild-type P0213-1 and of the selected mutants. Cultures were grown in synthetic cystic fibrosis medium (SCFM) at 37ºC, 180 rpm of orbital agitation, and OD_{640nm} was measured for 24 hours. Results are the means of data from two independent experiments.

According to figure 7, only two mutants present statistically significant differences in doubling time in comparison to the wild-type. The G38 mutant which presents an increase and F70 mutant which presents a decrease of the doubling time. Considering the disrupted gene of the G38 mutant, the higher doubling time presented by this mutant could be explained by the fact that bacterial cells cannot reset glutamate levels (due to its mutated gene and due to the consumption of all arginine in the medium in the first three hours of growth (12)). Without this reset, bacterial cells have more difficulty to produce some components essentials for growth, like amino acids, co-factors, among others, which originate from glutamate (34). The other mutant that presents a different doubling time, the F70 mutant, has a disrupted gene involved in the formation of an outer membrane protein. The lack of a functional outer membrane protein, in SCFM, had a positive effect in growth of this mutant (doubling time of 102.7 ± 5.1 min (data not shown)). Outer membranes porins were reported to be important in the uptake of nutrients, resistance to antibiotics, among others (35). However, the non-functional outer membrane porin of F70 mutant has not been characterized. Still, the STRING tool (36) identify some proteins related to the cell division that possibly interact with this protein.

Virulence determination in Galleria mellonella

To assess the virulence of the selected mutants and wild-type strain, *Galleria mellonella* was the chosen model of infection (Fig. 8).

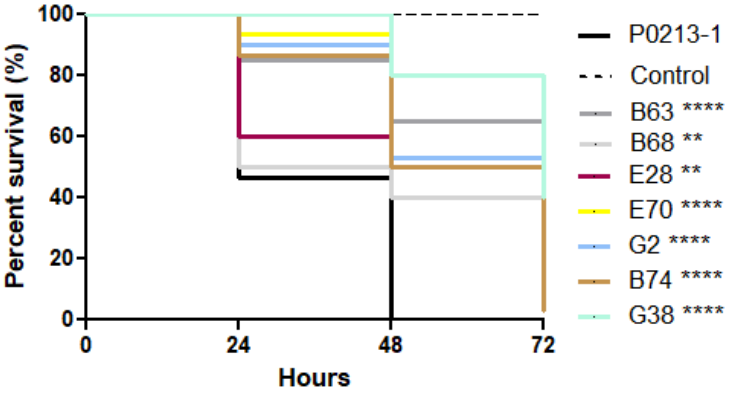

Fig. 8 Survival of *Galleria mellonella* larvae inoculated *with B. multivorans* (wild-type P0213-1 and the selected mutants which are statistically significant). Triplicate groups of 10 larvae were inoculated with each isolate and survival was followed for three days post-infection. Larvae were injected with approximately $1x10^4$ bacterial cells. The control experiment without bacteria is also represented. Statistical significance of differences between the Kaplan-Meier curve of the first isolate and the subsequent ones was determined: **, P-value < 0.01; ****, P-value < 0.0001.

Considering the first group of mutants reducing most of the biomass in the form of aggregates (B63, B68, E28, E36 and E50), all except E36 showed virulence attenuation when compared to the wild-type strain P0213-1. The one displaying higher attenuation is B63 mutant with xanthine dehydrogenase encoding gene disrupted. As already suggested before, this mutant might have defects in signaling pathways which would affect several cell traits, including virulence. *P. aeruginosa* deficient in (p)ppGpp and c-di-GMP showed virulence attenuation in a mouse model of infection (37).The second group of mutants producing smaller aggregates but in higher number than the wild-type strain (G2, H21, H42, E70 and F70) only G2, H42 and E70 mutants show significant virulence attenuation (Fig. 8).

In the third group which includes B74, E89 and G38, we have seen virulence attenuation in B74 and G38, but not E89 (Fig. 8). These mutants are the ones where most of the cells are free living. The exact mechanisms of reduced virulence that are dependent an S9 ribosomal protein or on a protein involved in nitrogen metabolism are unknown.

From our analysis we did not see any correlation between the type/number of aggregates formation and virulence in the chosen infection model.

Conclusion and future perspectives

The aim of this work was to explore the unknown mechanisms, responsible for the formation of this type of aggregates in bacteria through the construction of transposon library from a *B. multivorans* clinical isolate, P0213-1. Then, 13 selected mutants were characterized regarding several phenotypes like motility, exopolysaccharide production, virulence in *G. mellonella* and growth kinetics. The main objective was trying to interconnect some of these phenotypes with the ability to

form planktonic cellular aggregates and, consequently, to provide new possible mechanisms involved in the formation of cellular aggregates.

Although it was impossible to establish a linear relationship between each phenotype and aggregation ability, it is acceptable to assume that it was still possible to identify admissible players involved in the formation of aggregates by their role in the total set of tested phenotypes. Among that players are intracellular messengers (possibly (p)ppGpp and c-di-GMP and quorum sensing molecules), ribosomal proteins, outer membrane constituents and proteins involved in nitrogen metabolism. Considering the results obtained, as well as the information from previous studies, it is possible to infer that the two intracellular messengers ((p)ppGpp and c-di-GMP) may be the key to one of the mechanisms that act differentially in relation to the formation of the two types of biofilms considered in this study. Thus, it would have been important to better understand the role of each intracellular messenger in aggregates formation, quantifying each of them over time, and infer which pathways would have been influenced, for example, through transcriptomic analysis.

Based on the phenotypic results obtained with respect to the B74 mutant, it has been found that ribosomal proteins may be involved in other important processes in cells, in addition to their role in the ribosome assembly. Considering the results, it could be suggested a link between ribosomal proteins, cellular aggregation and motility. Point out further that this link was demonstrated before in *Bacillus subtillis*, but no kind of this association type was previously performed in gram-negative bacteria.

Also, quorum sensing system was might be important (B68 mutant and E70 mutant) for the triggering of aggregation. This association had previously been established in relation to the formation of biofilms. Thus, this result highlights the importance of cell communication in phenotypes such as cellular aggregation in which there is a large cellular community.

During this study many were the mutants that had disrupted genes related to proteins that are part of the cell membrane. One of the characteristics described as influencing the aggregate formation capacity is the cell surface properties, namely their charge. Under normal physiological conditions the cell surfaces have a net negative charge, however, it is known that this charge is highly variable and changes depending on the environment conditions and on the components that make up their surface. Bacteria may contain different surface structures such as fimbriae, lipopolysaccharides, hydrophobic amino acids or extracellular polymeric substances which in turn may contain glycoproteins, polysaccharides or even attached acids. These surface structures in solution will be charged and therefore the presence and nature of these surface appendages will alter the bacterial cell charge. Thus, in these mutants it should have been interesting to determine in what ways the gene disruption may lead to change in the aggregation phenotype through its influence on cell surface properties. To that end, the zeta potential of the bacterium that gives the information about the cell surface charge could have been relevant for the discussion of the results obtained in these mutants.

Despite the several players identified in this study as being involved in the formation of planktonic cellular aggregates, there is much more work to do to understand these complex structures. However, is important to highlight that the knowledge about cellular aggregates could be relevant to the development of potential therapeutics to improved treatments against *Bcc* bacteria.

References

1. Vasudevan R. 2014. Biofilms: Microbial Cities of Scientific Significance. J Microbiol Exp 1:1–16.
2. Moreau-Marquis S, Stanton BAB, O'Toole GGA. 2008. *Pseudomonas aeruginosa* biofilm formation in the cystic fibrosis airway. Pulm Pharmacol Ther 21:595–599.
3. Silva IN, Ramires MJ, Azevedo LA, Guerreiro AR, Tavares AC, Becker JD, Moreira LM. 2017. The regulator LdhR of *Burkholderia multivorans* plays a role in carbon overflow and in planktonic cellular aggregates formation. Appllied Environ Microbiol 83:e01343-17.
4. Cant N, Pollock N, Ford RC. 2014. CFTR structure and cystic fibrosis. Int J Biochem Cell Biol 52:15–25.
5. Saint-Criq V, Gray MA. 2017. Role of CFTR in epithelial physiology. Cell Mol Life Sci 74:93–115.
6. Lynch J. 2009. *Burkholderia cepacia* complex: impact on the cystic fibrosis lung lesion. Semin Respir Crit Care Med 30:569–610.
7. Hassett DJ, Sutton MD, Schurr MJ, Herr AB, Caldwell CC, Matu JO. 2009. *Pseudomonas aeruginosa* hypoxic or anaerobic biofilm infections within cystic fibrosis airways. Trends Microbiol 17:130–138.
8. Sriramulu DD, Lünsdorf H, Lam JS, Römling U. 2005. Microcolony formation: A novel biofilm model of *Pseudomonas aeruginosa* for the cystic fibrosis lung. J Med Microbiol 54:667–676.
9. Meade HM, Long SR, Ruvkun GB, Brown SE, Ausubel FM. 1982. Physical and genetic characterization of symbiotic and auxotrophic mutants of *Rhizobium meliloti* induced by transposon Tn5 mutagenesis. J Bacteriol 149:114–122.
10. J S, Russel DW. 2001. Molecular cloning: a laboratory manual. New York.
11. Altschul SF, Madden TL, Schäffer AA, Zhang J, Zhang Z, Miller W, Lipman DJ. 1997. Gapped BLAST and PSI-BLAST: A new generation of protein database search programs. Nucleic Acids Res 25:3389–3402.
12. Palmer KL, Aye LM, Whiteley M. 2007. Nutritional cues control *Pseudomonas aeruginosa* multicellular behavior in cystic fibrosis sputum. J Bacteriol 189:8079–8087.
13. Zlosnik JEA, Hird TJ, Fraenkel MC, Moreira LM, Henry DA, Speert DP. 2008. Differential mucoid exopolysaccharide production by members of the *Burkholderia cepacia* complex. J Clin Microbiol 46:1470–1473.
14. Ferreira AS, Leitao JH, Sousa SA, Cosme AM, Sa-Correia I, Moreira LM. 2007. Functional analysis of *Burkholderia cepacia* genes bceD and bceF, encoding a phosphotyrosine phosphatase and a tyrosine autokinase, respectively: role in exopolysaccharide biosynthesis and fiofilm formation. Appl Environ Microbiol 73:524–534.
15. Silva IN, Santos PM, Santos MR, Zlosnik JEA, Speert DP, Buskirk SW, Bruger EL, Waters CM, Cooper VS, Moreira M. 2016. Long-term evolution of *Burkholderia multivorans* during a chronic cystic fibrosis infection reveals shifting forces of selection. Am Soc Microbiol Journals 1:1–21.
16. Seed KD, Dennis JJ. 2008. Development of *Galleria mellonella* as an alternative infection model for the *Burkholderia cepacia* complex. Infect Immun 76:1267–75.
17. Sivapragasam S. 2015. Bacterial Xanthine Dehydrogenase Regulators.
18. Kanehisa M, Goto S. 2000. KEGG: Kyoto Encyclopedia of Genes and Genomes. Nucleic Acids Res 28:27–30.
19. Kulakova AN, Kulakov LA, Villarreal-Chiu JF, Gilbert JA,

McGrath JW, Quinn JP. 2009. Expression of the phosphonoalanine-degradative gene cluster from *Variovorax* sp. Pal2 is induced by growth on phosphonoalanine and phosphonopyruvate. FEMS Microbiol Lett 292:100–106.

20. Veselova MA, Lipasova VA, Zaitseva Y V., Koksharova OA, Chernukha MY, Romanova YM, Khmel' IA. 2012. Mutants of *Burkholderia cenocepacia* with a change in synthesis of N-acyl-homoserine lactones—Signal molecules of quorum sensing regulation. Russ J Genet 48:513–521.

21. Jassem AN, Forbes CM, Speert DP. 2014. Investigation of aminoglycoside resistance inducing conditions and a putative AmrAB-OprM efflux system in *Burkholderia vietnamiensis*. Ann Clin Microbiol Antimicrob 13:1–5.

22. Basler M. 2015. Type VI secretion system : secretion by a contractile nanomachine. Philos Trans B.

23. Chen R. 1975. The primary structure of protein S9 from the 30S subunit of *Echerichia*. FEBS Lett 52:139–140.

24. Lardi M, Aguilar C, Pedrioli A, Omasits U, Suppiger A, Cárcamo-Oyarce G, Schmid N, Ahrens CH, Eberl L, Pessi G. 2015. σ54-Dependent response to nitrogen limitation and virulence in *Burkholderia cenocepacia* strain H111. Appl Environ Microbiol 81:4077–4089.

25. Hashim S, Kwon DH, Abdelal A, Lu CD. 2004. The arginine regulatory protein mediates repression by arginine of the operons encoding glutamate synthase and anabolic glutamate dehydrogenase in *Pseudomonas aeruginosa*. J Bacteriol 186:3848–3854.

26. Schmid N, Suppiger A, Steiner E, Pessi G, Kaever V, Fazli M, Tolker-nielsen T, Jenal U, Eberl L. 2018. High intracellular c-di-GMP levels antagonize quorum sensing and virulence gene expression in *Burkholderia cenocepacia*. Microbiology 754–764.

27. Haaber J, Cohn MT, Frees D, Andersen TJ, Ingmer H. 2012. Planktonic aggregates of *Staphylococcus aureus* protect against common antibiotics. PLoS One 7:1–12.

28. Gupta KR, Kasetty S, Chatterji D. 2015. Novel functions of (p)ppGpp and cyclic di-GMP in mycobacterial physiology revealed by phenotype microarray analysis of wild-type and isogenic strains of *Mycobacterium smegmatis*. J Appl Environ Microbiol 81:2571–2578.

29. Dienerowitz M, Cowan L V., Gibson GM, Hay R, Padgett MJ, Phoenix VR. 2014. Optically trapped bacteria pairs reveal discrete motile response to control aggregation upon cell-cell approach. Curr Microbiol 69:669–674.

30. Takada H, Morita M, Shiwa Y, Sugimoto R, Suzuki S, Kawamura F, Yoshikawa H. 2014. Cell motility and biofilm formation in *Bacillus subtilis* are affected by the ribosomal proteins, S11 and S21. Biosci Biotechnol Biochem 78:898–907.

31. Liu Y, Lardi M, Pedrioli A, Eberl L, Pessi G. 2017. NtrC-dependent control of exopolysaccharide synthesis and motility in *Burkholderia cenocepacia* H111. PLoS One 12:1–22.

32. Bible AN, Khalsa-Moyers GK, Mukherjee T, Green CS, Mishra P, Purcell A, Aksenova A, Hurst GB, Alexandre G. 2015. Metabolic adaptations of *Azospirillum brasilense* to oxygen stress by cell-cell clumping and flocculation. Appl Environ Microbiol 81:8246–57.

33. Worlitzsch D, Tarran R, Ulrich M, Schwab U, Cekici A, Meyer KC, Birrer P, Bellon G, Berger J, Weiss T, Botzenhart K, Yankaskas JR, Randell S, Boucher RC, Döring G. 2002. Effects of reduced mucus oxygen concentration in airway *Pseudomonas* infections of cystic fibrosis patients. J Clin Invest 109:317–325.

34. Huaman MA, Fiske CT, Jones TF, Warkentin J, Shepherd BE, Maruri F, Sterling TR. 2015. The many roles of glutamate in metabolism. J Ind Microb Biotechnol 143:951–959.

35. Arhin A, Boucher C. 2010. The outer membrane protein OprQ and adherence of *Pseudomonas aeruginosa* to human fibronectin. Microbiology 156:1415–1423.

36. Szklarczyk D, Franceschini A, Wyder S, Forslund K, Heller D, Huerta-Cepas J, Simonovic M, Roth A, Santos A, Tsafou KP, Kuhn M, Bork P, Jensen LJ, Von Mering C. 2015. STRING v10: Protein-protein interaction networks, integrated over the tree of life. Nucleic Acids Res 43:D447–D452.

37. Xu X, Yu H, Zhang D, Xiong J, Qiu J, Xin R, He X, Sheng H, Cai W, Jiang L, Zhang K, Hu X. 2016. Role of ppGpp in *Pseudomonas aeruginosa* acute pulmonary infection and virulence regulation. Microbiol Res.

38. Dennis JJ, Zylstra GJ, Dennis JJ. 1998. Plasposons : modular self-cloning minitransposon derivatives for rapid genetic analysis of gram-negative bacterial genomes. Appl Environm Microbiol 64:2710–2715.

39. Kessler B, de Lorenzo V, Timmis KN. 1992. A general system to integrate lacZ fusions into the chromosomes of gram-negative eubacteria: regulation of the Pm promoter of the TOL plasmid studied with all controlling elements in monocopy. Mol Gen Genet 233:293–301.

Supplementary data

Table S1. Bacterial strains and plasmids

Strain or plasmid	Description	Reference or source
***Burkholderia multivorans* strains**		
P0213-1	Cystic fibrosis isolate, Canada	D.P. Speert University of British Columbia
B63	P0213-1 derivative with the plasposon pTn*Mod*-Km^r, inserted in *xdHA_3* gene	This study
B68	P0213-1 derivative with the plasposon pTn*Mod*-Km^r, inserted in *fadR* gene	This study
B74	P0213-1 derivative with the plasposon pTn*Mod*-Km^r, inserted in *rpsI* gene	This study
E28	P0213-1 derivative with the plasposon pTn*Mod*-Km^r, inserted in *pphA_2* gene	This study
E36	P0213-1 derivative with the plasposon pTn*Mod*-Km^r, inserted in *nemR*_2 gene	This study
E50	P0213-1 derivative with the plasposon pTn*Mod*-Km^r, inserted in a MMPL family protein gene	This study
E70	P0213-1 derivative with the plasposon pTn*Mod*-Km^r, inserted in *ppsA* gene	This study
E89	P0213-1 derivative with the plasposon pTn*Mod*-Km^r, inserted in *cycA_3* gene	This study
F70	P0213-1 derivative with the plasposon pTn*Mod*-Km^r, inserted in an outer membrane porin precursor gene	This study
G2	P0213-1 derivative with the plasposon pTn*Mod*-Km^r, inserted in *ttgR_3* gene	This study
G38	P0213-1 derivative with the plasposon pTn*Mod*-Km^r, inserted in *gltB_1* gene	This study
H21	P0213-1 derivative with the plasposon pTn*Mod*-Km^r, inserted in *clpB_1* gene	This study
H42	P0213-1 derivative with the plasposon pTn*Mod*-Km^r, inserted in *ypeA* gene	This study
P0213-1/PMF18-4	P0213-1 overexpressed with plasmid PMF18-4	This study
B74/pBBR1MCS	B74 with vector pBBR1MCS	This study
B74/PMF18-4	B74 complemented with plasmid PMF18-4	This study
P0213-1/pBBR1MCS	P0213-1 with vector pBBR1MCS	This study
***E. coli* strains**		
JM109	F´ *traD36 proA$^+$B$^+$ lacI^q Δ(lacZ)M15/ Δ(lac-proAB) glnV44*	Promega
DH5-α	DH5α *recA1*, *lacUi69*, *o80dlacZ ΔM15*	Gibco BRL
Plasmids		
pTn*Mod*Ωkm	Carring a Km^r Plasposon with pMB1oriR	(38)
pRK600	ColE1 oriV; RP4tra$^+$ RP4oriT; Cm^r; helper in triparental matings	(39)

Table S2. Primers used in this work.

Primers	
pTnModΩKm - fw	5' GCAGAGCGAGGTATGTAGGC '3
pTnModΩKm - rev	5' TTATGCCTCTTCCGACCATC '3
KmR	5' CCTTTTTACGGTTCCTGGCCT '3
OriR	5' GTGCAATGTAACATCAGAG '3
Pro_rplM - fw	5' GGGGTACCGAAATGGCGAACGCGCTC 3'
Pro_rplM - rev	5' GGAATTCCATATGTGCGGAAAAGCCCTGAATTATAA 3'
rpsI - fw	5' GGAATTCCATATGATCGGTAACTGGAACTACGGTACG 3'
rpsI - rev	5' GCTCTAGAAAGCTTTAGCCGCTATTGTAGGG 3'

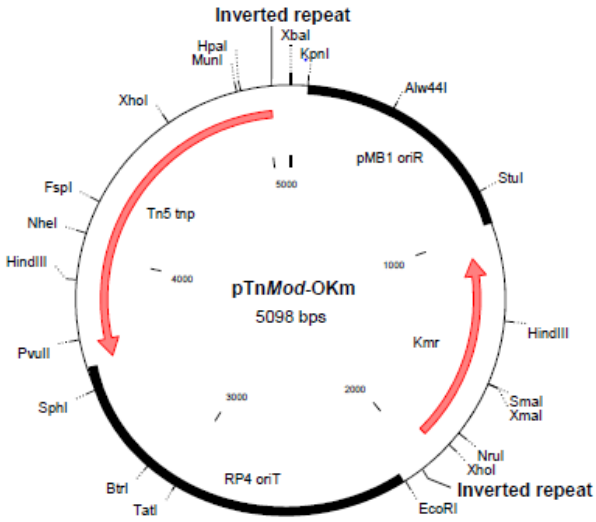

Fig. S1 Physical map of transposon pTn*Mod*ΩKm (38)**.** Transposon is composed of genes that encode a transponase, two inverted repeats and a selectable marker, in this case, a kanamycin marker. The sequence between inverted repeats is the unique part of transposon that remain inserted in genome. The size is about 2000 bp.